# Larger aggregates of mutant seipin in Celia's Encephalopathy, a new protein misfolding neurodegenerative disease

Alejandro Ruiz-Riquelme[a], Sofía Sánchez-Iglesias[a], Alberto Rábano[b], Encarna Guillén-Navarro[c], Rosario Domingo-Jiménez[d], Adriana Ramos[a,†], Isaac Rosa[a,f], Ana Senra[a], Peter Nilsson[e], Ángel García[a,f], David Araújo-Vilar[a,g*] and Jesús R. Requena[a,g*]

[a]CIMUS Biomedical Research Institute, University of Santiago de Compostela-IDIS, 15782 Santiago de Compostela, Spain
[b]Neuropathology Department and Tissue Bank, Fundación CIEN, 28031 Madrid, Spain
[c]Section of Medical Genetics and Dysmorphology, Division of Pediatrics, Hospital Clínico Universitario Virgen de la Arrixaca, IMIB-Arrixaca. 30120 Murcia; UCAM-Catholic University of Murcia; CIBERER-ISCIII, Madrid, Spain
[d]Section of Neuropediatrics, Division of Pediatrics, Hospital Clínico Universitario Virgen de la Arrixaca, IMIB-Arrixaca. 30120 Murcia; CIBERER-ISCIII, Madrid, Spain
[e]Affinity Proteomics, SciLifeLab, School of Biotechnology, KTH – Royal Institute of Technology, SE 171-21Stockholm, Sweden
[f]Department of Pharmacology, University of Santiago de Compostela, 15782 Santiago de Compostela, Spain
[g]Department of Medicine, University of Santiago de Compostela, 15782 Santiago de Compostela, Spain

[†]Present address: Department of Psychiatry and Behavioural Sciences, The Johns Hopkins University School of Medicine, Baltimore, MD 21287, USA.

*To whom correspondence should be addressed at: Room SS1D, CIMUS Biomedical Research Institute, University of Santiago de Compostela-IDIS, 15782 Santiago de Compostela, Spain Tel: +34 881815464; Email: jesus.requena@usc.es (J.R.R.); U.E.T.e.M, Lab 3, 2nd floor, CIMUS Biomedical Research Institute, University of Santiago de Compostela-IDIS, 15782 Santiago de Compostela, Spain. Tel: +34 881815426; Email: david.araujo@usc.es (D.A.V.)

## Abstract

Celia's Encephalopathy (MIM #615924) is a recently discovered fatal neurodegenerative syndrome associated with a new *BSCL2* mutation (c.985C>T) that results in an aberrant isoform of seipin (Celia seipin). This mutation is lethal in both homozygosity and compounded heterozygosity with a lipodystrophic *BSCL2* mutation, resulting in a progressive encephalopathy with fatal outcomes at age 6-8. Strikingly, heterozygous carriers are asymptomatic, conflicting with the gain of toxic function attributed to this mutation. Here we report new key insights about the molecular pathogenic mechanism of this new syndrome. Intranuclear inclusions containing mutant seipin were found in brain tissue from a homozygous patient suggesting a pathogenic mechanism similar to other neurodegenerative diseases featuring brain accumulation of aggregated, misfolded proteins. Sucrose gradient distribution showed that mutant seipin forms much larger aggregates as compared with wild type (wt) seipin, indicating an impaired oligomerization. On the other hand, the interaction between wt and Celia seipin confirmed by coimmunoprecipitation (CoIP) assays, together with the identification of mixed oligomers in sucrose gradient fractionation experiments can explain the lack of symptoms in heterozygous carriers. We propose that the increased aggregation and subsequent impaired oligomerization of Celia seipin leads to cell death. In heterozygous carriers, wt seipin might prevent the damage caused by mutant seipin through its sequestration into harmless mixed oligomers.

## Keywords

Seipin; *BSCL2*; Neurodegeneration; Lipodystrophy; Intranuclear inclusions; Progressive encephalopathy; Celia's encephalopathy; Oligomerization; Phenotype rescue.

## Introduction

Seipin is an endoplasmic reticulum (ER) resident protein highly expressed in brain and testicles (Windpassinger et al., 2004). It has 3 isoforms of 462, 398 and 287 amino acids (Cartwright and Goodman, 2012). Its predicted structure would encompass two transmembrane domains, a conserved core region and both amino- and carboxi- termini facing the cytoplasm (Lundin et al., 2006).

The function of seipin remains incompletely understood. There are evidences for a role of seipin in lipid droplet (LD) synthesis (Fei et al., 2011 Szymanski et al., 2007 and Yang et al., 2013a) and adipocyte differentiation (Payne, 2008, Yang, 2013a and Yang, 2013b). Previous studies have shown the existence of seipin oligomers of about 9 subunits in yeast related to the synthesis of lipid

droplets (Binns et al., 2010). In addition, oligomers of 12 subunits have also been described for human seipin (Sim et al., 2013a).

Recently, new roles for seipin in nervous tissue have been proposed. Seipin might regulate excitatory synaptic transmission by modulating AMPA receptor levels (Wei et al., 2013) and synaptic vesicle exocytosis by directly regulating synaptic vesicle docking (Wei et al., 2014). Furthermore, a role for seipin in the mobilization of lipids to the developing brain has also been proposed (Hötta-Vuori et al., 2013).

Mutations in the *Seipin/BSCL2* gene cause either type 2 congenital generalized lipodystrophy (CGL2) (Magré et al., 2001) or dominant motor neuron diseases (Windpassinger et al., 2004). However, we recently reported on a novel mutation in the *BSCL2* gene (c.985C>T) that results in a fatal neurodegenerative syndrome (Guillén-Navarro et al., 2013) henceforward called "Celia's Encephalopathy" (MIM #615924). This mutation induces an alternative splicing event that results in skipping of exon 7 and a reading frame shift giving place to a new aberrant protein, hereafter called Celia seipin.

To date, six patients have been identified. Two of them are homozygous for the c.985C>T mutation whereas the other four are compound heterozygous, carrying the c.985C>T mutation plus a lipodystrophic mutation (c.538G>T or c.507_511del). Both homozygous and compound heterozygous patients showed a similar neurological course, suffering from progressive encephalopathy starting at age 2-3, with a fatal outcome at age 6-8. Strikingly, heterozygous carriers are asymptomatic, conflicting with the gain of toxic function attributed to the mutation (Guillén-Navarro et al., 2013).

The pathogenic mechanism by which Celia seipin exerts its pathogenic effect is not completely understood. Our previous work has shown high expression level of BiP, an ER stress marker, in Celia seipin-overexpressing compared to control cells (Guillén-Navarro et al., 2013). ER stress has been extensively associated to several neurodegenerative diseases (Matus et al., 2011). Besides, we found ubiquitin positive intranuclear inclusions in the hypothalamus of the index case (Guillén-Navarro et al., 2013). Ubiquitin positive intranuclear inclusions have been associated to other neurodegenerative syndromes like Huntington's disease (Sieradzan et al., 1999).

Likewise, ER stress has been demonstrated in the N88S and S90L mutations of the seipin gene, both of which lead to motor neuropathies (Ito and Suzuki, 2007 and Ito et al. 2008). Moreover, cytoplasmic inclusion bodies with a cytoprotective function have been detected in association to these mutations (Ito et al., 2008 and Ito et al., 2012).On the other hand, mild mental retardation has been reported linked to CGL2 (Van Maldergem et al., 2002) suggesting an

impairment of brain functions of seipin. However, considering the short term lethal nature of Celia's Encephalopathy, a different or more aggressive pathogenic mechanism has to be involved in this new disease.

The results reported here provide new insights about the molecular mechanism involved in Celia's Encephalopathy.

## Materials and Methods

This study was approved by the local Ethics Review Panel of Xunta de Galicia (Spain) and was in accordance with the Declaration of Helsinki. Patient's relatives gave informed consent for participation in the study and publication of clinical and biochemical information.

### Tissue samples

Hypothalamus, and parietal and occipital cortex samples were obtained from the homozygous index case during autopsy, from two control cases (both of them males, 43 and 68 years at death, respectively) deceased by suicide, and from one control case (female, 6 years at death) deceased from an abdominal tumor, with autopsy performed in accordance with the Spanish legislation.

Adipose tissue samples were obtained by biopsy of the abdominal area from a homozygous patient (index case), at 6 years of age, and from an age-matched healthy control. Small pieces of visceral adipose tissue were placed on a 60 mm dish (BD Falcon™, Mississauga, ON, Canada) containing Dulbecco's modified Eagle's medium (DMEM) (Sigma-Aldrich, St. Louis, MO, USA) plus 30% fetal bovine serum (FBS) (Gibco, Life Technologies, Gaithersburg, MD, USA) and 50 µg/ml gentamicin (Sigma-Aldrich), and incubated at 37 ºC with 5% $CO_2$ in a Water-Jacket $CO_2$ incubator (NuAire, Plymouth, MN, USA). Preadipocytes were recognised by the presence of small lipid droplets in the fibroblast-like cells. Preadipocytes were tripsinized with TrypLE™ Express Stable Trypsin-like Enzyme with Phenol Red (Gibco) and cultured on 100 mm dishes in DMEM containing 10% FBS and 1% penicillin-streptomycin (Invitrogen, Carlsbad, CA, USA).

### Cell culture and transfection

HeLa, 3T3, HEK293 and COS-7 cells were grown in Dulbecco's modified Eagle's medium (DMEM) (Sigma-Aldrich) supplemented with 10% FBS (Gibco), 1% penicillin/streptomycin (Invitrogen) and 1% L-glutamine (Gibco). SH-SY5Y cells were grown in 1:1 Ham's F12:Earle's Balanced Salt Solution (Sigma-Aldrich) supplemented with 15% FBS (Gibco), 1% penicillin/streptomycin (Invitrogen), 1% L-glutamine (Gibco) and 1% non-essential amino-acids (NEAA)

(Gibco). Transfections were performed with TurboFect (Thermo-Fisher Scientific, Waltham, MA, USA) or Fugene 6 (Promega, Fitchburg, WI, USA) according to the manufacturer's instructions.

cDNA

A plasmid containing wild type human seipin fused to a myc tag (6 myc-wt seipin pCS2+MT) was a kind gift from D. Ito, Keio University, Japan. Myc fused Celia seipin expression plasmid were previously described (Guillén-Navarro et al., 2013).

Plasmids containing wild type or Celia seipin fused to a FLAG tag were created as follows: seipin cDNA was amplified by PCR using primers designed for human wt seipin (forward: 5'-GCCGAATTCATGTCTACAGAAAAGGTAGACCA-3'; reverse: 5'-GCCTCTAGAGGAACTAGAGCAGGTGGGG-3') and Celia seipin (forward: 5'-GCCGAATTCATGTCTACAGAAAAGGTAGACCA-3'; reverse: 5'-GCCTCTAGAGGGGCTGCTGATCTGGTTT-3'), then digested with the restriction enzymes EcoRI (Thermo-Fisher Scientific) and XbaI (Thermo-Fisher Scientific), purified and inserted into p3XFLAG-CMV-14 (Sigma-Aldrich) plasmid. Correct cloning was verified by sequencing. Control plasmids were empty p3XFLAG-CMV-14 (Sigma-Aldrich) and pCS2+MT.

Antibodies

The following primary antibodies were used in this study: anti seipin (HPA042394) rabbit polyclonal antibody (1:40-1:500, The Human Protein Atlas [Uhlen, 2010]), anti c-myc (9E10) mouse monoclonal antibody (1:1000, Santa Cruz Biotechnology, Dallas, TX, USA), anti-FLAG rabbit polyclonal antibody (1:1000, Sigma-Aldrich), anti-GAPDH (1:10000-1:20000, Sigma-Aldrich), anti-Tubulin (1:5000, Sigma-Aldrich), anti BiP (1:1000, Cell Signaling), anti 14-3-3 pan (Thermo-Fisher Scientific). The following secondary antibodies were used: Alexa Fluor 555- conjugated anti-mouse IgG secondary antibody (Invitrogen), horseradish peroxidase-linked anti mouse IgG secondary antibody (GE Healthcare UK, Buckinghamsire, UK), horseradish peroxidase-linked anti rabbit IgG secondary antibody (Dako, Glostrup, Denmark).

Density gradient fractionation

Lysates (*vide infra*) from HeLa cells transfected with Myc-wt, Myc-Celia or both seipin isoforms (10:1 proportion) were loaded on the top of 10-60 % sucrose gradients (sucrose dissolved in PBS) (Supplementary Material, Fig. S3A) and centrifuged at 272109 g in a SW60Ti rotor (Beckmann Coulter, Brea, CA, USA), 16 h, 4ºC.

8 fractions of 325 µl were collected from the top, subjected to SDS-PAGE and analyzed by immunoblotting with 1:1000 anti c-myc (9E10) antibody (Santa Cruz Biotechnology) followed by incubation with horseradish peroxidase-linked secondary antibody (GE Healthcare).

The MW of the oligomers was estimated using the theoretical MW of Myc-wt seipin (58 kDa) and Myc-Celia seipin (46 kDa). According to the calibration curve (Supplementary Data, Fig. S3B) Myc-wt seipin oligomers have a MW of approximately 690 kDa. Dividing the estimated MW of Myc-wt seipin oligomers and the MW of each subunit we can conclude that the oligomers are composed of 12 subunits (690/58 = 11.89). Myc-Celia seipin aggregates have a MW of 1250-2000 kDa, being composed of between 27 and 44 subunits. This estimation is the result of 3 independent assays.

Western Blot analysis

HeLa cells were transfected with Myc-wt seipin, Myc-Celia seipin or empty vector. After 48 hours, cells were lysed in RIPA buffer (50 mM Tris-HCl, pH 7.2, 150 mM NaCl, 1% NP-40, 0.5% sodium deoxycholate, 0.1% SDS, 1mM PMSF, 1mM DTT, 10 µg/ml leupeptin and 10 µg/ml aprotinin). Protein content was determined by using the Bio-Rad protein assay (Bio-Rad laboratories, Hercules, CA, USA). Protein samples were separated by SDS-PAGE and transferred to a PVDF transfer membrane (Millipore, Billerica, MA, USA). The membrane was probed with primary antibodies and subsequently with horseradish peroxidase-linked secondary antibodies.

Immunoblots showed in Figure 2A and 2B were scanned and analyzed by densitometry using the Image J 1.48v software (National Institutes of Health, Bethesda, MD, USA). All blots shown are representative of a minimum of 3 experiments.

*BSCL2* expression study

Total RNA was extracted from lymphocytes and reverse-transcribed as previously reported (Victoria et al., 2010). *BSCL2* cDNA PCR details are available upon request. Expression of *BSCL2* mRNA was quantified in a Light Cycler 2.0 (Roche Diagnostics, Sant Cugat del Vallés, Spain) using specific probes and oligonucleotide primers designed by Universal Probe Library (Roche Diagnostics) (Supplementary Data, Fig. S4B). Results were normalized to the RNA polymerase II and 18s genes, using the $2^{-\Delta\Delta\ CT}$ method (Livak and Schmittgen, 2001).

Co-immunoprecipitation

Lysates (*vide supra*) from transfected HeLa cells were subjected to coimmunoprecipitation using the Pierce c-Myc Tag IP/Co-IP Kit (Thermo-Fisher Scientific) according to the manufacturer's instructions. 500 μg of lysates were incubated in spin columns with anti c-Myc agarose overnight at 4ºC. Myc immunoprecipitates were eluted with non-reducing sample buffer, boiled for 5 min, separated by SDS-PAGE and analyzed by immunoblotting with 1:1000 anti c-Myc antibody.

Immunohistochemistry

Paraffin sections of the posterior hypothalamus, at a coronal level including the mammillary body, and parietal and occipital cortices of the homozygous index case and of three control cases (two of them males, 43 and 68 years at death, respectively, and one female child, 6 years at death) were immunostained with anti-seipin antibody HPA042394 (The Human Protein Atlas). Primary antibody was incubated at 1:40-1:500 dilutions and heat-induced antigen retrieval was performed by pressure cooker heating using PT-Link (Dako). Staining was amplified and revealed by means of the Dako Envision system (Dako).

Immunostaining and confocal imaging

HeLa, SH-SY5Y, HEK293, COS7 and 3T3 cells were grown in EZ Millicell slides (Millipore) and transfected with Myc-wt seipin, Myc-Celia seipin or empty vector. After 48 h, cells were fixed with 1:1 Methanol-Acetone for 20 min at -20 ºC and permeabilized in 0.5% Triton X-100. Non-specific binding was blocked with 5% BSA. Slides were incubated with 1:1000 anti c-myc (9E10) antibody (Santa Cruz Biotechnology) at 4ºC overnight. The next day, after four washes, the slides were incubated with Alexa Fluor 555 (Thermo-Fisher Scientific) conjugated anti mouse secondary antibody and DAPI stain (Sigma-Aldrich) for 1 hour in darkness and mounted. Immunofluorescence staining was examined a Leica TCS SP5 confocal microscope and LAS AF Software (Leica, Mannheim, Germany).

Proteomic analysis

Proteomic analysis of preadipocytes was performed using high-resolution two-dimensional gel electrophoresis (2-DE) for protein separation and matrix-assisted laser desorption/ionization mass spectrometry (MALDI/MS) or nanoflow liquid chromatography-electrospray ionization-tandem mass spectrometry (nLC-MS/MS) for the analysis of selected differentially regulated protein spots. Further details are available in Supplementary Data, S6.

## Results

Celia seipin forms intranuclear aggregates in the brain

Our previous work showed the presence of intranuclear ubiquitin-positive inclusions in the brain of the index case, likely to contain misfolded, aggregated mutant seipin.

To confirm the presence of seipin in these intranuclear ubiquitin positive inclusions we performed an immunohistochemistry study. Tissue samples from different brain regions from the index case (homozygous for the c.985C>T mutation) were probed with anti-seipin (Supplementary Data, Fig. S1) and anti-ubiquitin antibodies. We observed several scattered positively stained intranuclear inclusions in neurons of the posterior hypothalamic nuclei (Fig. 1A-C) and the parietal and occipital cortices (Supplementary Data, Fig. S2A-B) of the patient. As previously reported (Guillén-Navarro et al., 2013) ubiquitin-reactive intranuclear inclusions were also frequently observed in neurons (Fig. 1B). These inclusions were mostly single and round-shaped, although occasional multiple inclusions were also observed. Some of the ubiquitin-reactive inclusions were recognized by the seipin-specific antibody; ubiquitin-reactive inclusions were found in a higher number probably because of a higher sensibility of the anti-ubiquitin antibody. No neuronal nuclear inclusions were identified in the control cases (Fig. 1D & Supplementary Data, Fig. S2C-D).

Celia seipin exhibits aberrant oligomerization status

It has been shown that human wt seipin forms oligomers of 12 subunits (Sim et al., 2013a). At least for the yeast seipin homolog *FLD1*, these oligomers are involved in the generation of lipid droplets at the ER-LD junctions (Szymanski et al., 2007). We reasoned that mutated seipin might fail to assemble correctly. Instead, aberrant aggregation would result in the observed inclusions.

To test this hypothesis, protein extracts from HeLa cells overexpressing Myc-wt or Myc-Celia seipin were subjected to fractionation in 10 to 60% sucrose density gradients (Supplementary Data, Fig. S3A). Fractions of 325 µl were collected and analyzed by western blot (WB) (Fig. 2A).
Wt seipin mainly appears in fraction 6. According to the calibration curve (Supplementary Data, Fig. S3B), this corresponds to a molecular weight (MW) of ~690 kDa which means that wt seipin is made up of oligomers of ~12 subunits. In contrast, Celia seipin mainly appears in fraction 8, which suggests that it forms much larger aggregates under similar conditions. These results suggest impaired oligomerization/aggregation of Celia seipin.

Both Celia and wt seipin are localized at the ER/nucleus continuum

The fact that aberrant aggregates pf Celia seipin appear in the nucleus begs the question of how a protein that is theoretically located in the ER can reach that localization. However, previous studies have shown that mutant seipin can appear in a ring surrounding the cell nucleus (Payne et al., 2008, Sim et al., 2013a). This has been confirmed for A212P and L61P mutations, both of which lead to classic lipodystrophy, although this perinuclear localization has only been observed in C3H10T1/2 cells. On the other hand, we have previously detected, by microscopy and subcellular fractionation, the presence in the nuclear fraction of both wt and Celia seipin (Guillén-Navarro et al., 2013). Because of the continuity between the ER membrane and the outer nuclear envelope (Goyal et al., 2013 and Mauger, 2012), a perinuclear localization for an ER protein like seipin is not unreasonable. Perinuclear localization of Celia seipin would be consistent with the observed intranuclear deposition of aberrant aggregates.

By immunofluorescence, we compared the subcellular localization of wt and Celia seipin in 5 different cell lines: HeLa, SH-SY5Y, 3T3, HEK293 and COS7. Both seipin isoforms appeared surrounding the nucleus in addition to their normal cytoplasmatic localization (Fig. 3).

*BSCL2* expression levels in heterozygous carriers

Our previous findings point to a gain of toxic function for the new aberrant protein Celia seipin. Therefore, the absence of symptoms observed in heterozygous carriers for the c.985C>T mutation is strikingly paradoxical. We hypothesized that interaction of wt with Celia seipin might inhibit aberrant aggregation of the latter in heterozygous individuals, thus rescuing the disease phenotype. We therefore quantitated expression levels of RNA corresponding to both seipin isoforms in two heterozygous carriers (parents of the index case) by real time RT-PCR (Supplementary Data, S4A), to assess their relative abundance, as a first step to validate our hypothesis. We found a 10:1 ratio of wt seipin to Celia seipin (Fig. 4A). The difference with the expected Mendelian ratio of 1:1 might be explained by the degradation of the majority of the conceivably less stable Celia seipin mRNA, by nonsense-mediated mRNA decay (NMD), as suggested for other mutations (Frischmeyer & Dietz, 1999, Caputi, 2002). While our results were obtained in lymphocytes, it is reasonable to extrapolate them to brain, where a vast excess of wt seipin over Celia seipin would facilitate a protective neutralization of Celia seipin if wt seipin were able to interact with it.

To complete a comprehensive picture of the expression of different *BSCL2* transcripts, we compared expression of wt seipin in lymphocytes of

heterozygous carriers and healthy homozygous controls, which was found to be 35%, slightly lower but overall consistent with the expected 50% (Fig. 4B).

Celia seipin and wt seipin interact with one another

The interaction between wt and mutant forms of seipin has been proved in previous studies (Fei et al., 2011). To assess whether Celia and wt seipin can interact we developed a coimmunoprecipitation assay. HeLa cells were co-transfected with both FLAG-wt seipin and Myc-Celia seipin at two different ratios: 1:1 and 10:1 (wt:Celia), the latter ratio simulating the expression levels found in heterozygous carriers. Lysates were immunoprecipitated with anti c-myc agarose and the precipitate probed with an anti-FLAG antibody.

Interaction between wt and Celia seipin was observed at both 1:1 and 10:1 ratios (Fig. 5 & Supplementary Data, Fig. S5). At a 10:1 ratio, though, the intensity of FLAG-wt seipin bands (corresponding to FLAG-wt seipin trapped in Myc-Celia precipitates) was higher than that seen at a 1:1 ratio. In this experiment, as samples were boiled in Laemli buffer prior to electrophoresis separation, tagged seipin appeared as several bands corresponding to monomers (shown in Fig. 5), partially dissociated oligomers and high MW aggregates, (Supplementary Data, Fig. S5) as previously described (Fei et al., 2011, Yang et al., 2013a). These results clearly confirm the interaction between wt seipin and Celia seipin.

Identification of wt-Celia seipin mixed oligomers

Once their interaction was confirmed, we proceeded to assess whether wt and Celia seipin might be capable of forming mixed oligomers, recruiting Celia seipin into mixed, normal size oligomers, thus impeding their aggregation into larger, presumably toxic, oligomers. We therefore expressed wt and Celia seipin at a 10:1 ratio in HeLa cells and performed density gradient ultracentrifugation of cell extracts. We found a change in the pattern of distribution of Celia seipin when co-expressed with a 10:1 excess of wt seipin. More specifically, the flotation pattern of Celia seipin was found to mimic that of wt seipin (Fig. 2B–D). This result clearly indicates the interaction between both seipin isoforms through the formation of mixed oligomers.

Proteomic analysis of preadipocytes from a homozygous patient

To further investigate the molecular changes that might be provoked by Celia seipin we performed a proteomic analysis. The analysis was carried out in preadipocytes, as we reasoned that this would allow us to detect early

pathogenic changes, as opposed to the terminal changes that might be encountered in brain tissue obtained at necropsy.

Proteomic identification of differentially regulated proteins in preadipocytes from the index case as compared with an age-matched healthy control was performed. The analysis was based on two-dimensional gel electrophoresis (2-DE) and mass spectrometry (Supplementary Data, S6). We set a fold change threshold for differentially regulated features of > 2. Several differentially regulated protein spots ($p < 0.05$) were found (Supplementary Data, Fig. S5). Of them, we were able to identify 32 corresponding to 20 differentially regulated open-reading frames (ORFs) (Table 1). We verified by WB changes in expression of BiP/GRP78 (also known as "78 kDa glucose related protein"), and 14-3-3γ (Supplementary Data, S7).

The differentially regulated protein dataset was characterized using PANTHER (Mi et al., 2010) protein classes (Supplementary Data, S8). Proteins belonging to PANTHER classes "oxidoreductase" (25% of differentially regulated proteins) and "chaperone" (20% of differentially regulated proteins) were predominant in preadipocytes from the index case.

GO-BP and GO-MF categories were assessed in the differentially regulated protein dataset using DAVID Bioinformatics Resources v6 (Dennis et al., 2003 and Huang et al., 2009). GO-BP categories significantly overrepresented ($p< 0.05$) were summarized using REVIGO (Supek et al., 2011). Enrichment in GO-BP categories related to cellular stress ("cellular response to reactive oxygen species"), cytoskeleton regulation ("negative regulation of actin filament depolimerization"), or apoptosis ("negative regulation of apoptotic processes" or "release of cytochrome c from mitochondria") and GO-MF term "oxidoreductase activity" was found in preadipocytes from the index case.

## Discussion

Mutations in *BSCL2* have been traditionally associated with lipodystrophy (loss of function mutations), and, more recently, with neuro-motor syndromes (gain of toxic function mutations), all of them non-lethal diseases in the short term. However, the appearance of a fatal neurodegenerative syndrome caused by a new seipin mutation suggests unknown pathogenic mechanisms to be associated to this protein.

Here, we report new clues that cast more light about the pathogenicity observed in Celia's Encephalopathy, offering also an explanation of the lack of symptoms in heterozygous carriers.

First, we have confirmed that the ubiquitin positive intranuclear inclusions observed in different brain regions from the index case contain Celia seipin. Second, we have demonstrated an impaired oligomerization of Celia seipin, forming large aggregates. Third, we have obtained new evidence showing that a fraction of seipin is naturally located in the nucleus. Fourth, we have demonstrated the interaction between wt and Celia seipin resulting in the formation of mixed oligomers. And fifth, we have found significant changes in some key pathways and biological processes in preadipocytes from the index case, suggesting increased reticulum stress.

The immunohistochemical analysis of hypothalamus, and paritetal and occipital cortices from the index case has confirmed that the ubiquitin positive intranuclear inclusions previously observed contain seipin. These inclusions are likely to form because of the impaired oligomerization and aggregation of Celia seipin. Neuronal intranuclear inclusions have been found in several neurodegenerative diseases like Huntington's disease (Davies et al., 1997). In fact, the pattern of distribution of intranuclear inclusions, present only in a few cells in specific brain locations, typical of Huntington´s disease (Margulis and Finkbeiner, 2014), is very reminiscent of what we observe in our case. Of note, seipin has been found to be up-regulated in proteomic analyses of Parkinson's disease (PD) patients in both substantia nigra (Licker et al., 2014) and locus coeruleus (Van Dijk et al., 2011). Interestingly, in the same way as seipin, α-synuclein, a protein that aggregates in PD, has been related to lipid droplet synthesis (Cole et al., 2002), supporting a possible link between PD and Celia's Encephalopathy.

On the other hand, cytoplasmic inclusion bodies with a neuroprotective function have been described for N88S and S90L mutations (Ito et al., 2008 and Ito et al., 2012); a similar protective function of Celia Seipin intranuclear inclusions cannot be ruled out at this point and merits further investigation.

Previous studies have shown the existence of interaction between wt seipin and some mutant seipin forms (N88S and A212P) (Fei et al., 2011, Sim et al., 2013a). Self-interaction of wt seipin has also been demonstrated (Fei et al., 2011). In fact, there is experimental evidence suggesting that human seipin forms oligomers of 12 subunits (Sim et al., 2013a), while yeast seipin forms 9-mers (Binns et al., 2010). By density gradient fractionation we have confirmed the existence of wt seipin oligomers of ~12 subunits. In contrast, Celia seipin showed impaired oligomerization, forming large aggregates. It should be kept in mind that the analytical approach used (density gradient fractionation) has some limitations. Detergent molecules present in the solubilization buffer and bound to seipin oligomers, might lead to a slight overestimation of their MW. Furthermore, they might alter their flotation properties. Therefore, the estimated MWs should be considered with caution. Of note, when fractionation was

carried out in a gradient including the same concentration of detergent present in the samples (1% NP-40, 0.1% SDS) similar results were obtained (data not shown). However, the fact that a value of 12 units has been obtained for wt seipin oligomers, in agreement with previous estimations obtained by other methods, (Sim et al., 2013a) supports the overall soundness of the method. In any case, a different flotation pattern is clearly observed in Celia seipin with respect to wt seipin, independently of their absolute MWs, which allows us to conclude that Celia seipin forms abnormal, larger aggregates.

The severe neurodegenerative phenotype showed by homozygous patients carrying the c.985C>T mutation (Guillén-Navarro et al., 2013), together with the finding of inclusions containing Celia seipin and the impaired oligomerization provoked by the mutation points to a gain of toxic function in Celia´s encephalopathy. Therefore, heterozygous carriers would be expected to suffer some degree of pathology caused by the expression of a small amount of Celia seipin (Fig. 4A and Supplementary Data, Fig. S4A). Strikingly, they are completely asymptomatic. This contradiction might be explained by a threshold effect according to which a higher amount of Celia seipin than that expressed in heterozygous carriers would be necessary to exert a toxic effect. Nevertheless, the existence of compound heterozygous patients carrying Celia´s mutation together with other lipodistrophic seipin mutations (c.538G>T or c.507_511del) and showing the same phenotype as homozygous patients (Guillén-Navarro et al., 2013), rules out such a threshold effect. Carrying a single copy of the mutant allele is sufficient to develop the disease, suggesting a more complex pathogenic molecular mechanism.

Given the 10:1 wt/Celia seipin ratio found in heterozygous carriers (Fig. 4A), we hypothesized that wt seipin might co-opt Celia seipin units into mixed oligomers of a normal size, thus preventing their aberrant aggregation.

We have been able to confirm an interaction of FLAG-wt and Myc-Celia seipin by coimmunoprecipitation. This interaction was observed at both a 1:1 and a 10:1 ratio (wt:Celia). In addition, by density gradient fractionation we observed a change in the buoyancy pattern of Celia seipin at a 10:1 ratio of Myc-wt/Myc-Celia seipin. Specifically, at a 10:1 ratio Celia seipin migrates at a lighter fraction than when alone, mimicking the behavior of wt seipin (Fig. 2B–D). This suggests that wt seipin is able to “drag” Celia seipin into mixed oligomers changing its flotation pattern. This finding clearly supports the existence of interaction between wt and Celia seipin through mixed oligomers (Fig. 6). Because of the absence of wt seipin, in compound heterozygous patients, this proposed phenotype rescue would not be possible.
Our results are reminiscent of prevention of aggregation of N88S and S90L seipin mutants when coexpressed with wt seipin (Fei et al., 2011), and,

inversely, of the failure of wt seipin to form normal oligomers in the presence of an excess of A212P mutant seipin (Sim et al., 2013a).
The presence of Celia seipin aggregates in nuclear inclusions begs the question of how a presumed ER protein (Cartwright and Goodman, 2012) ends up in that localization. In a previous study we demonstrated by both subcellular fractionation and confocal immunofluorescence microscopy in HeLa cells that seipin, besides localizing to the ER, is also present in a nuclear/perinuclear localization (Guillén-Navarro et al., 2013). Here, by a more comprehensive confocal immunofluorescence microscopy study in different cell lines, we confirm that both wt and Celia seipin are located surrounding the nucleus, most probably in the nuclear envelope.

The outer nuclear membrane is continuous with the ER and contains several proteins in common with it (Goyal and Blackstone, 2013, Mauger, 2012). Because of this, a masking effect of the ER located seipin over the perinuclearly located seipin may have occurred in previous immunofluorescence studies. Methanol/Acetone fixation, used in our study, avoids this problem by precipitating perinuclearly located seipin on the nuclear envelope, unmasking and rendering it more available for antibody detection (http://microscopy.duke.edu/sampleprep/if.html [Accessed January 8, 2015]).

On the other hand, given the proposed role for seipin in lipid droplet synthesis and adipogenesis it is noteworthy the recently described existence of nuclear lipid droplets (Layerenza et al., 2013). Seipin could be related to these structures in a similar way that it is related to classic lipid droplets.

In order to explore early pathogenic alterations, we carried out an unbiased proteomic study of preadipocytes from the index case. Results highlight the role of antioxidant activity and cellular stress in Celia's Encephalopathy. Differential regulation of oxidoreductases may be caused by an increase in oxidative stress in preadipocytes. Increased antioxidant enzyme activity has been extensively related to other neurodegenerative diseases (Lin and Beal, 2006).

Chaperones are also differentially regulated in the homozygous patient, in agreement with the function attributed to this class of proteins in response to cellular stress. The verification by WB of a differential regulation for BiP/GRP78, a chaperone that functions as ER stress marker and regulates protein folding (Dudek et al., 2009), suggests a role for ER stress in the pathogenic mechanism of Celia's Encephalopathy. A differential regulation of 14-3-3γ protein has also been verified. Interestingly, 14-3-3γ protein targets misfolded chaperone-associated proteins to aggresomes (Xu et al., 2013). Therefore, the differential regulation of both chaperones and 14-3-3γ could be part of an attempt of the cell machinery to deal with accumulation of misfolded Celia seipin in the ER through aggregation. On the other hand, the differential regulation of

some chaperones (e.g. Heat shock cognate 71 kDa protein or BiP/GRP78) being a side-effect caused by their accumulation in aggregates (Waelter et al., 2001) cannot be ruled out. Such aggregates are most likely insoluble, therefore not contributing to the sample submitted to proteomic assays. It should be noted, however, that aggregates have not been observed yet in preadipocytes. Neither they were seen in Celia seipin-overexpressing HeLa cells. These cells do not seem to recapitulate the development of intranuclear inclusions, as observed in neurons from the index case. However, this is not surprising given the fast dilution effect resulting from cell division.

Strikingly, cytoskeleton regulation is also affected in preadipocytes from the index case. Bearing in mind the proposed role for seipin in cytoskeleton remodeling during adipogenesis (Yang et al., 2013b) a possible adverse effect of Celia seipin aggregation in this route would not be surprising.

Taking together our results, we propose a central role of Celia seipin aggregation in the pathogenesis of Celia´s Encephalopathy. Aberrant aggregation, with subsequent formation of intranuclear inclusions and ER stress would lead to widespread brain damage. In asymptomatic carriers, interaction of excess wt seipin with Celia seipin, co-opting it to normal oligomers, would prevent the damage. Thus, Celia´s Encephalopathy appears as a new member of the class of neurodegenerative diseases associated to deposition of protein aggregates in the brain, such as Alzheimer´s disease, Parkinson´s disease, Huntington´s disease, frontotemporal dementias or prion diseases.

## Acknowledgements

The name Celia´s encephalopathy is a tribute to Celia´s memory and was chosen in agreement with her parents, to whom we are deeply indebted for their collaboration and commitment to research. We thank Ana Senra, CIMUS Biomedical Research Institute, for assistance with histopathology, Dr. Justin Rochford for his suggestions and advice and Dr. Daisuke Ito for kindly providing the Myc-wt seipin plasmid. This work was supported by Instituto de Salud Carlos III (grant number PI 10/02873and PI13/00314), European Regional Development Fund, FEDER, Xunta de Galicia (grant number 10PXIB208013PR) and Fundación MEHUER. AG acknowledges support from the Spanish Ministry of Economy and Competitiveness (grant number SAF2013-45014-R). ARR is the recipient of an IDIS pre-doctoral fellowship. SSI is a Research Fellow granted by the Asociación Española de Familiares y Afectados de Lipodistrofias (AELIP)

## Conflict of Interest Statement

None declared.

## References


Binns, D., Lee, S., Hilton, C.L., Jiang, Q.X. and Goodman, J.M., 2010. Seipin is a discrete homooligomer. Biochemistry, 49, 10747–10755

Caputi, M., Kendzior, R.J., and Beemon, K.L., 2002. A nonsense mutation in the fibrillin-1 gene of a Marfan syndrome patient induces NMD and disrupts an exonic splicing enhancer. Genes Dev., 16, 1754–1759

Cartwright, B.R. and Goodman, J.M., 2012. Seipin: from human disease to molecular mechanism. J. Lipid. Res., 53, 1042–1055

Cole, N.B., Murphy, D.D., Grider, T., Rueter, S., Brasaemle, D. and Nussbaum, R.L., 2002. Lipid droplet binding and oligomerization properties of the Parkinson's disease protein alpha-synuclein. J. Biol. Chem., 277, 6344–6352

Davies, S.W., Turmaine, M., Cozens, B.A., DiFiglia, M., Sharp, A.H., Ross, C.A., Scherzinger, E., Wanker, E.E., Mangiarini, L. and Bates, G.P., 1997. Formation of neuronal intranuclear inclusions underlies the neurological dysfunction in mice transgenic for the HD mutation. Cell, 90, 537–48

Dennis, G., Jr., Sherman, B. T., Hosack, D.A., Yang, J., Gao, W., Lane, H.C., Lempicki, R.A., 2003. DAVID: database for annotation, visualization, and integrated discovery. Genome Biol., 4, P3.

Dudek, J., Benedix, J., Cappel, S., Greiner, M., Jalal, C., Müller, L. and Zimmermann, R., 2009. Functions and pathologies of BiP and its interaction partners. Cell. Mol. Life Sci., 66, 1556–1569

Fei, W., Li, H., Shui, G., Kapterian, T.S., Bielby, C., Du, X., Brown, A.J., Li, P., Wenk, M.R., Liu, P. et al., 2011. Molecular characterization of seipin and its mutants: implications for seipin in triacylglycerol synthesis. J. Lipid. Res., 52, 2136–2147

Frischmeyer, P.A. and Dietz, H.C., 1999. Nonsense-mediated mRNA decay in health and disease. Hum. Mol. Genet., 8, 1893–1900

Goyal, U. and Blackstone, C., 2013. Untangling the web: mechanisms underlying ER network formation. Biochim. Biophys. Acta, 1833, 2492–2498.

Guillén-Navarro, E., Sánchez-Iglesias, S., Domingo-Jiménez, R., Victoria, B., Ruiz-Riquelme, A., Rábano, A., Loidi, L., Beiras, A., González-Méndez, B.,

Ramos, A. et al. 2013. A new seipin-associated neurodegenerative syndrome. J. Med.Genet., 30, 401–409

Han, S., Bahmanyar, S., Zhang, P., Grishin, N., Oegema, K., Crooke, R., Graham, M., Reue, K., Dixon, J.E., and Goodman, J.M., 2012. Nuclear envelope phosphatase 1-regulatory subunit 1 (formerly TMEM188) is the metazoanSpo7p ortholog and functions in the lipin activation pathway. J. Biol. Chem., 287, 3123–3137.

Hötta-Vuori, M., Salo, V.T., Ohsaki, Y., Suster, M.L. and Ikonen, E., 2013. Alleviation of seipinopathy-related ER stress by triglyceride storage. Hum. Mol. Genet., 22, 1157–1166

Huang, D.W., Sherman, B.T. andLempicki, R.A., 2009. Systematic and integrative analysis of large gene lists using DAVID bioinformatics resources. Nat. Protocols, 4, 44–57.

Ito, D. and Suzuki, N., 2007. Molecular pathogenesis of Seipin/BSCL2 related motor neuron diseases. Ann. Neurol., 61, 237–250

Ito, D. et al., 2008. Characterization of seipin/BSCL2, a protein associated with spastic paraplegia 17. Neurobiol. Dis. 31, 266–277

Ito, D., Yagi, T., Ikawa, M. and Suzuki, N., 2012. Characterization of inclusion bodies with cytoprotective properties formed by seipinopathy-linked mutant seipin. Hum. Mol. Genet., 21, 635–646.

Jeninga, E.H., De Vroede, M.,Hamers, N., Breur, J.M., Verhoeven-Duif, N.M., Berger, R., Kalkhoven, E., 2012. A patient with congenital generalized lipodystrophy due to a novel mutation in BSCL2: indications for secondary mitochondrial dysfunction. JIMD reports, 4, 47–54

Layerenza, J.P., González, P., García de Bravo, M.M., Polo, M.P., Sisti, M.S. and Ves-Losada, A., 2013. Nuclear lipid droplets: A novel nuclear domain. Biochim. Biophys. Acta, 1831, 327–340

Licker, V., Turck, N., Kövari, E., Burkhardt, K., Côte, M., Surini-Demiri, M., Lobrinus, J.A., Sánchez, J.C. and Burkhard, P.R., 2014. Proteomic analysis of human substantia nigra identifies novel candidates involved in Parkinson’s disease pathogenesis. Proteomics, 14, 784–794

Lin, M.T. and Beal, M.F., 2006. Mitochondrial dysfunction and oxidative stress in neurodegenerative diseases. Nature, 443, 787–795

Livak, K.J. andSchmittgen, T.D., 2001. Analysis of relative gene expression data using real-time quantitative PCR and the 2-$\Delta\Delta^{CT}$ method. Methods, 25, 402–408

Lundin, C., Nordström, R., Wagner, K., Windpassinger, C., Andersson, H., Von Heijne, G. and Nilsson, I., 2006. Membrane topology of the human seipin protein. FEBS Lett., 580, 2281–2284

Magré, J., Delépine, M., Khallouf, E., Gedde-Dahl, T., Van Maldergem, L., Sobel, E., Papp, J., Meier, M., Mégarbané, A., Bachy, A. et al., 2001. Identification of the gene altered in Berardinelli-Seip congenital lipodystrophy on chromosome 11q13. Nat. Genet. 28, 365–370

Margulis, J. and Finkbeiner, S., 2014. Proteostasis in striatal cells and selective neurodegeneration in Huntington's disease. Front. Cell. Neurosci. 8, 218

Matus, S., Glimcher, L.H., and Hetz, C., 2011. Protein folding stress in neurodegenerative diseases: a glimpse into the ER. Curr. Opin. Cell. Biol., 23, 239–252

Mauger, J.P., 2012. Role of the nuclear envelope in calcium signaling. Biol. Cell., 104, 70–83

Mi, H., Dong, Q., Muruganujan, A., Gaudet, P., Lewis, S. and Thomas, P.D., 2010. PANTHER version 7: improved phylogenetic trees, orthologs and collaboration with the Gene Ontology Consortium. Nucleic Acids Res., 38, D204–D210.

Payne, V.A., Grimsey, N., Tuthill, A., Virtue, S., Gray, S.L., Dalla Nora, E., Semple, R.K., O'Rahilly, S. and Rochford, J.J., 2008. The human lipodystrophy gene BSCL2/Seipin may be essential for normal adipocyte differentiation. Diabetes. 57, 2055–2060

Shevchenko, A., Wilm, M., Vorm, O. and Mann, M., 1996. Mass spectrometric sequencing of proteins silver-stained polyacrylamide gels. Anal Chem., 68, 850–858.

Sieradzan, K.A., Mechan, A.O., Jones, L., Wanker, E.E., Nukina, N. and Mann, D.M., 1999. Huntington's disease intranuclear inclusions contain truncated, ubiquitinated huntingtin protein. Exp. Neurol. 156, 92–99

Sim, M.F.M., Talukder, M.M.U., Dennis, R.J., O'Rahilly, S., Edwarson, J.M. and Rochford, J.J., 2013a. Analysis of naturally occurring mutations in the

human lipodystrophy protein seipin reveals multiple potential pathogenic mechanisms. Diabetologia, 56, 2498–2506

Sim, M.F.M., Dennis, R.J., Aubry, E.M., Ramanathan, N., Sembongi, H., Saudek, V., Ito, D., O'Rahilly, S., Siniossoglou, S. and Rochford, J.J., 2013b. The human lipodystrophy protein seipin is an ER membrane adaptor for the adipogenic PA phosphatase lipin 1. Mol. Metab. 2, 38–46

Supek, F., Bošnjak, M., Škunca, N. and Šmuc, T., 2011. REVIGO summarizes and visualizes long lists of Gene Ontology terms. PLoS ONE, 6, e21800

Szymanski, K.M., Binns, D., Bartz, R., Grishin, N.V., Li, W.P., Agarwal, A.K., Garg, A., Anderson, R.G., and Goodman, J.M., 2007. The lipodystrophy protein seipin is found at endoplasmic reticulum lipid droplet junctions and is important for droplet morphology. Proc. Natl. Acad. Sci. U.S.A., 104, 20890–20895

Uhlen, M., Oksvold, P., Fagerberg, L., Lundberg, E., Jonasson, K., Forsberg, M., Zwahlen, M., Kampf, C., Wester, K., Hober, S. et al., 2010. Towards a knowledge-based Human Protein Atlas. Nat. Biotechnol. 28 (12): 1248–50

Van Dijk, K.D., Berendse, H.W., Drukarch, B., Fratantoni, S.A., Pham, T.V., Piersma, S.R., Huisman, E., Brevé, J.J.P., Groenewegem, H.J., Jiménez, C.R. et al., 2012. The proteome of the locus ceruleus in Parkinson's disease: relevance to pathogenesis. Brain Pathology, 22, 485–498

Van Maldergem, L., Magré, J., Khallouf, T.E., Gedde-Dahl, T., Delépine, M., Trygstad, O., Seemanova, E., Stephenson, T., Albott, C.S., Bonnici, F. et al., 2002. Genotype-phenotype relationships in Berardinelli-Seip congenital lipodystrophy. J. Med. Genet., 39, 722–733

Victoria, B., Cabezas-Agricola, J.M., González-Méndez, B., Lattanzi, G., Del Coco, R., Loidi, L., Barreiro, F., Calvo, C., Lado-Abeal, J. and Araújo-Vilar, D., 2010. Reduced adipogenic gene expression in fibroblasts from a patient with type 2 congenital generalized lipodystrophy. Diabetic Medicine, 27, 1178–1187

Waelter, S., Boeddrich, A., Lurz, R., Scherzinger, E., Lueder, G., Lehrach, H. and Wanker, E.E., 2001. Accumulation of mutant huntingtin fragments in aggresome-like inclusion bodies as a result of insufficient protein degradation. Mol. Biol. Cell, 12, 1393–1407

Wei, S., Soh, S.L., Qui, W., Yang, W., Seah, C.J., Guo, J., Ong, W.Y., Pang, Z.P. and Han, W., 2013. Seipin regulates excitatory synaptic transmission in cortical neurons. J. Neurochem., 124, 478–489

Wei, S., Soh, S.L., Xia, J., Ong, W.Y., Pang, Z.P. and Han, W., 2014. Motor neuropathy-associated mutation impairs Seipin functions in neurotransmission. J. Neurochem., 129, 328–338

Wen, Z., Nguyen, H.N., Guo, Z., Lalli, M.A., Wang, X., Su, Y., Kim, N.S., Yoon, K.J., Shin, J., Zhang, C. et al., 2014. Synaptic dysregulation in a human iPS cell model of mental disorders. Nature, 515, 414–418

Windpassinger, C., Auer-Grumbach, M., Irobi, J., Patel, H., Petek, E., Hörl, G., Malli, R., Reed, J.A., Dierick, I., Verpoorten, N. et al., 2004. Heterozygous missense mutations in the BSCL2 gene cause distal hereditary motor neuropathy and Silver syndrome. Nat. Genet., 36, 271–276

Yang, W., Thein, S., Guo, X., Xu, F., Venkatesh, B., Sugii, S., Radda, G.K. and Han, W., 2013a. Seipin differentially regulates lipogenesis and adipogenesis through a conserved core sequence and an evolutionary acquired C-terminus. Biochem. J., 452, 37–44

Yang, W., Thein, S., Wang, X., Bi, X., Ericksen, R.E., Xu, F. and Han, W., 2013b. BSCL2/seipin regulates adipogenesis through actin cytoskeleton remodeling. Hum. Mol. Genet., 23, 502–513

Xu, Z., Graham, K., Foote, M., Liang, F., Rizkallah, R., Hurt, M., Wang, Y., Wu, Y. and Zhou, Y., 2013. 14-3-3 protein targets misfolded chaperone-associated proteins to aggresome. J. Cell Sci., 126, 4173–4186

**Web References**

Duke University Medical Center, Light Microscopy Core Facility. http://microscopy.duke.edu/sampleprep/if.html
(Accessed January 8, 2015)

**Legends to figures**

**Figure 1**. **Immunohistochemical staining for seipin and ubiquitin in pathological and control cases. A-B**: High magnification images of neuronal intranuclear inclusions in hypothalamus from a homozygous patient, reactive to seipin (HPA042394) (**A**) and to ubiquitin (**B**) antibodies. **C-D**: Low magnification images of the posterior hypothalamus of a homozygous patient (**C**) and a control case (**D**). The higher seipin-reactivity observed in neuronal bodies in the

control case compared with the homozygous patient could be caused by the lower expression level of Celia seipin. Scale bar: 100 μm.

**Figure 2. Density gradient fractionation of wt and Celia seipin**. Homogenates of HeLa cells overexpressing (**A**) wt or Celia seipin and (**B**) wt and Celia seipin co-expressed at a 10:1 (wt:Celia) ratio were subjected to sucrose gradient fractionation. (**C**) Percentage of seipin in each gradient fraction, as determined by scanning of WBs. (**D**) Higher exposure time image of the band with MW = 50 in panel B (expression 10:1, wt:Celia).

**Figure 3. Subcellular localization of seipin in several cell lines**. HeLa, 3T3, SH-SY5Y, HEK293 and COS7 cells grown on coverslips were transfected with wt seipin, Celia seipin or empty vector, immunostained with anti c-Myc (9E10) and imaged by confocal microscopy. Nuclei were stained with DAPI.

**Figure 4. *BSCL2* expression levels in healthy heterozygous carriers.** (**A**) Percentage of wt and Celia seipin in lymphocytes from heterozygous carriers. Total RNA extracted from lymphocytes was analyzed by real time RT-PCR. Wt seipin was measured as *BSCL2* bearing exon 7 transcript whereas Celia seipin was measured as exon 7 skipped *BSCL2* transcript (Supplementary Data, S3A–B). (**B**) Percentage of wt seipin in lymphocytes from heterozygous carriers compared to non-carriers (wt/wt). The difference to 100 % corresponds to a naturally expressed seipin isoform (287 aas) indistinguishable of Celia seipin through RT-PCR.

**Figure 5. Wt and Celia seipin interact**. Equal amounts of lysates from transfected HeLa cells were immunoprecipitated with anti c-myc and examined for coimmunoprecipitation of FLAG-wt seipin by immunoblotting. Lysates were previously probed with antibodies to confirm the validity of the transfection.

**Figure 6. Proposed model for the pathogenic mechanism of Celia seipin in homozygotes (A) and phenotype rescue in heterozygous carriers (B).** Please read the text for details.

**Table 1. List of differentially regulated proteins when comparing preadipocytes from the index case vs. control.**

**Figure 1**

Click here to download high resolution image

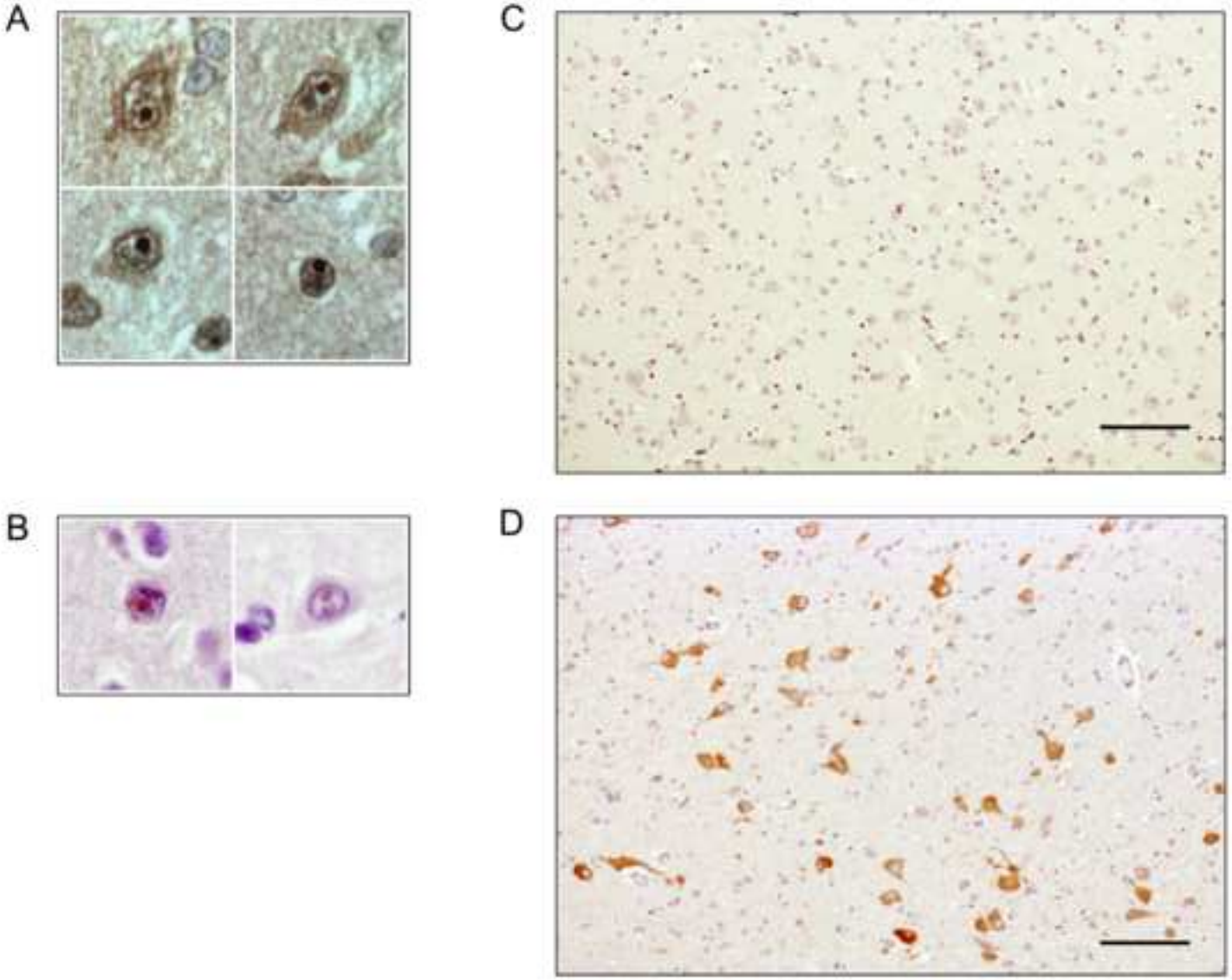

**Figure 2**

Click here to download high resolution image

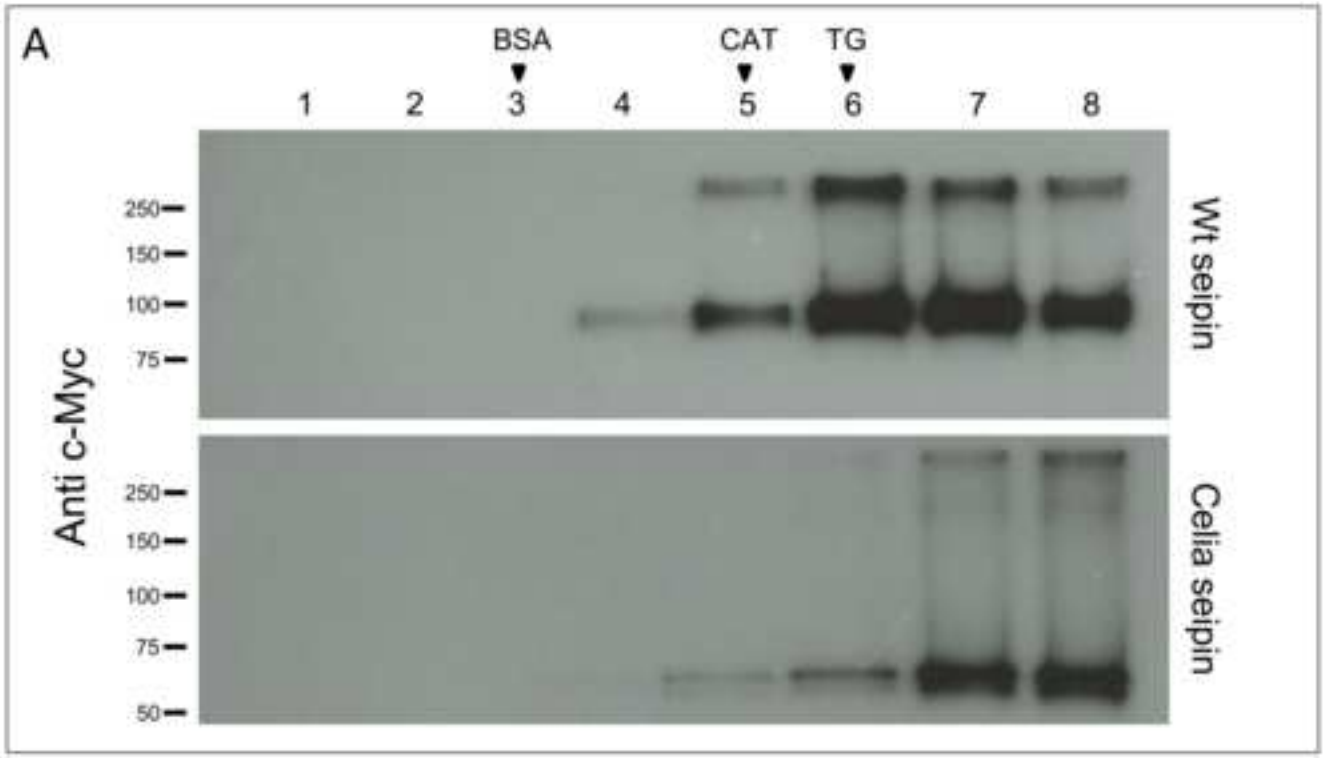


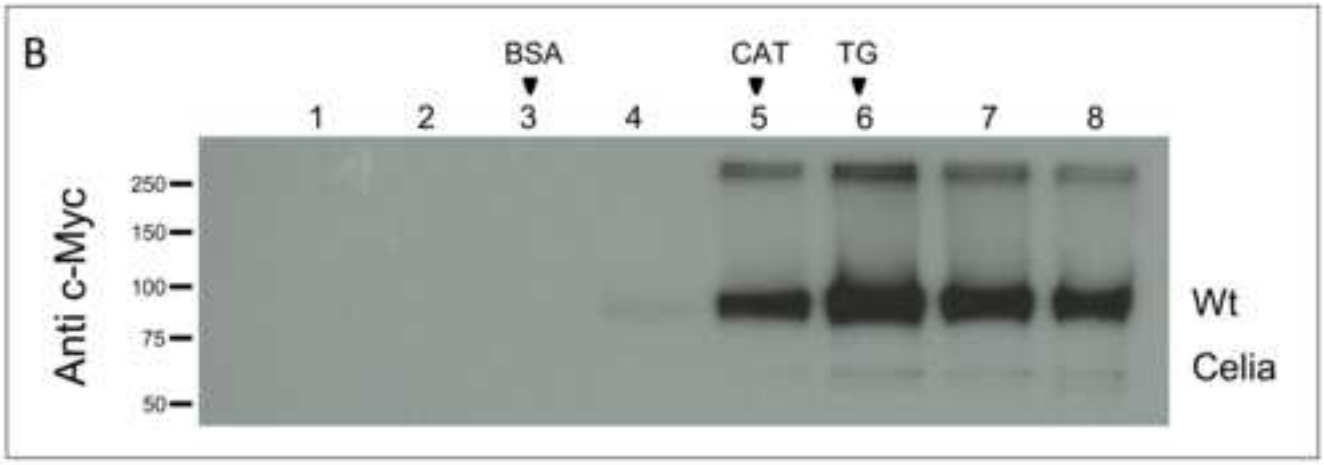


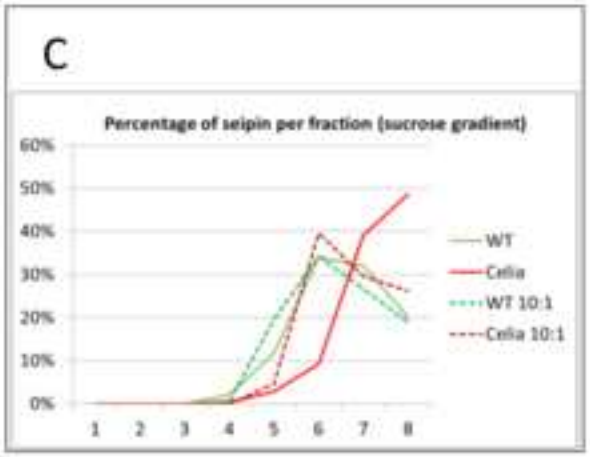


**Figure 3**

**Click here to download high resolution image**

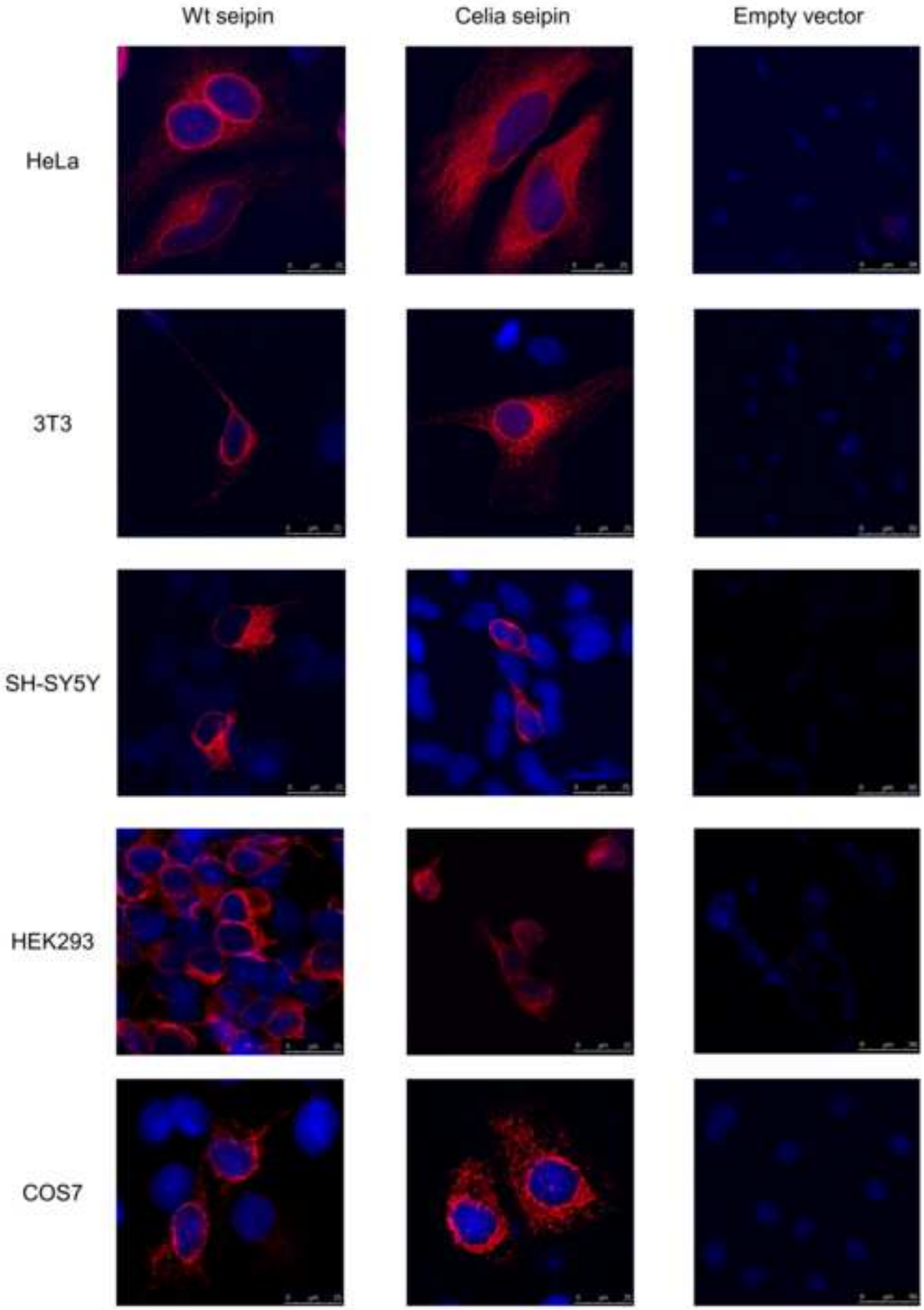

**Figure 4**

Click here to download high resolution image

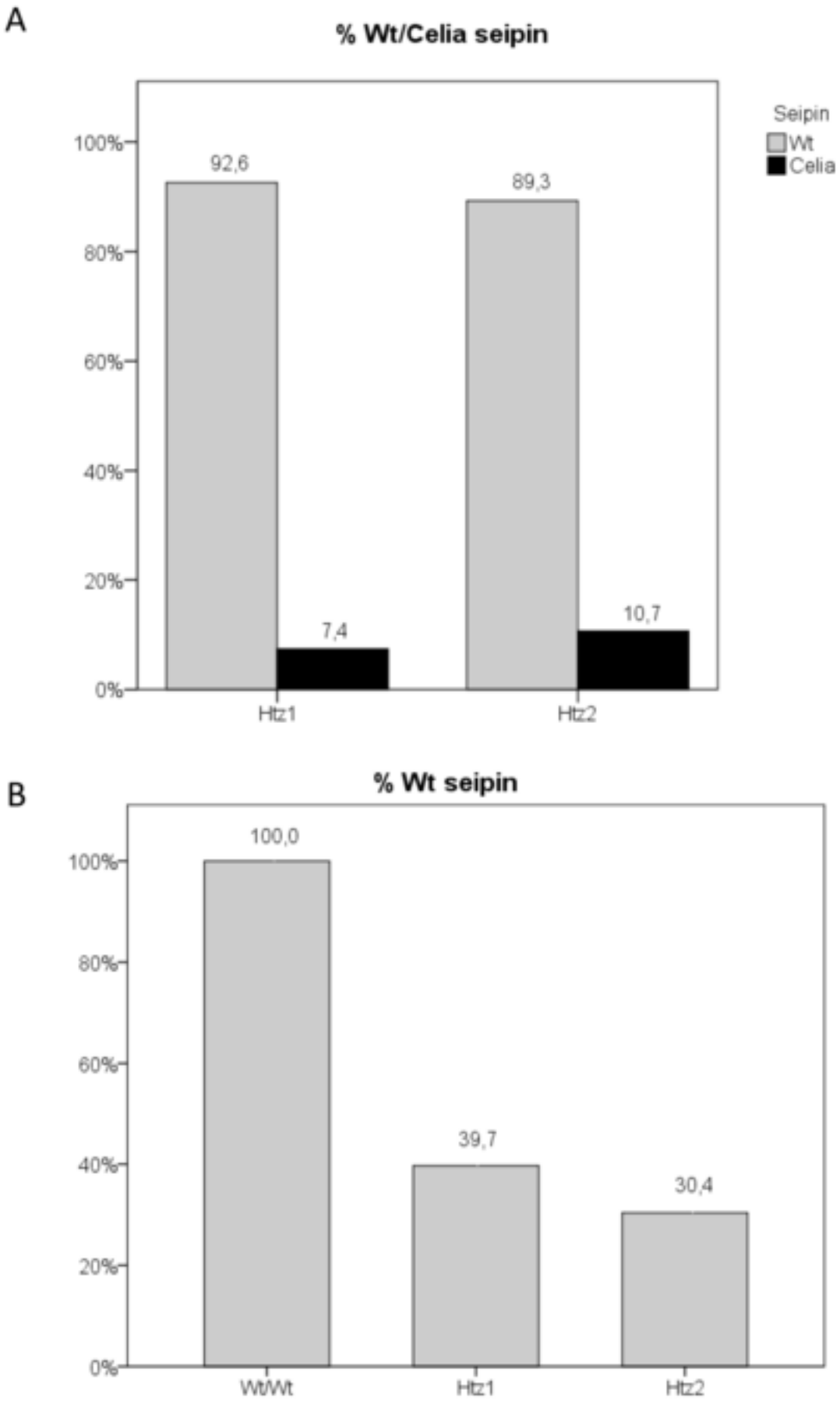

**Figure 5**

Click here to download high resolution image

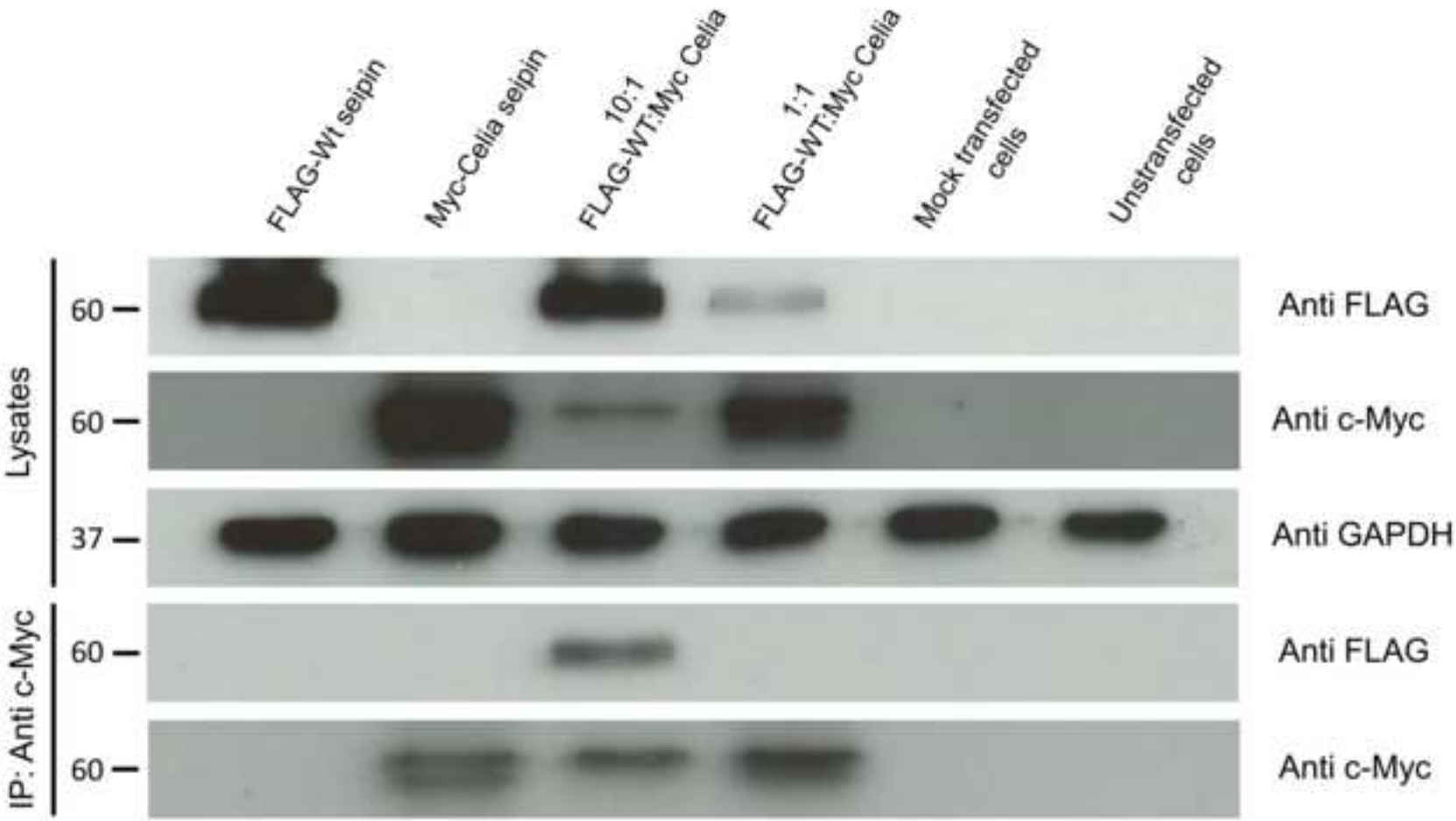

**Figure 6**

Click here to download high resolution image

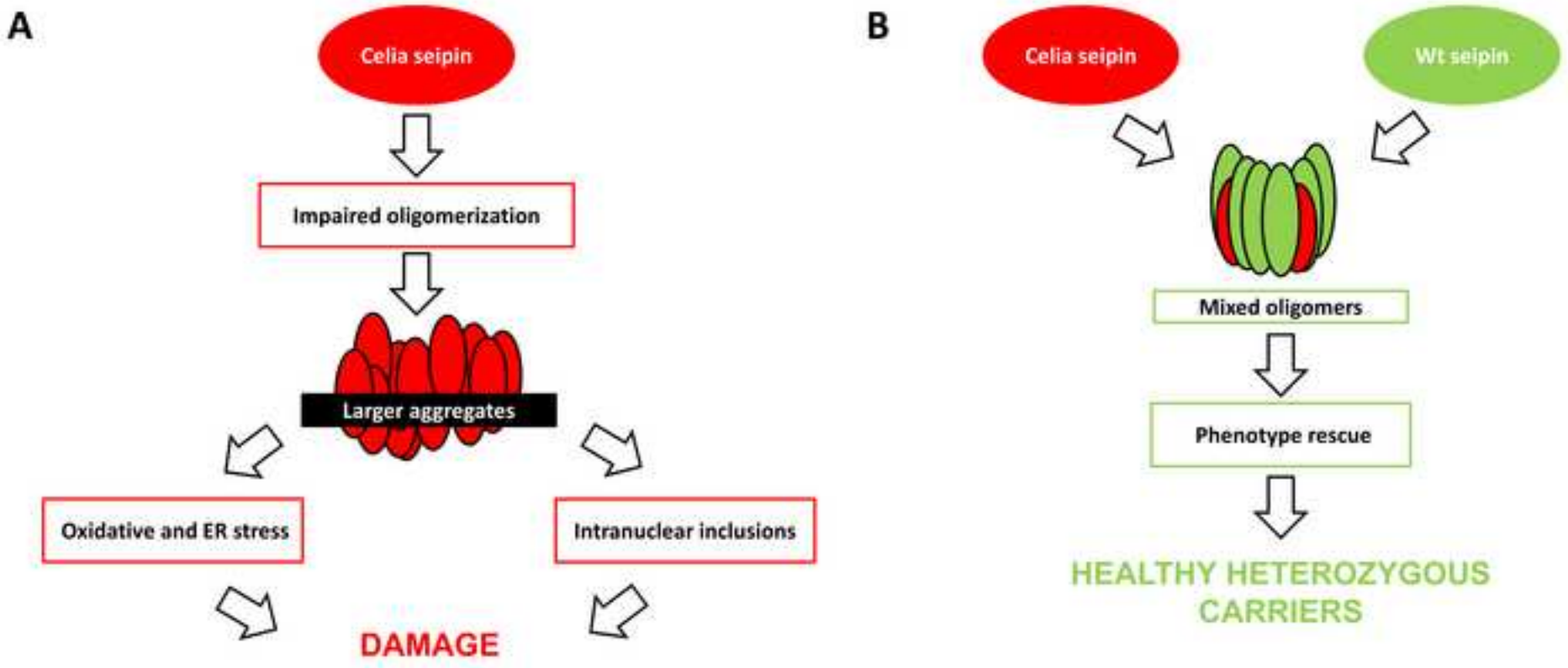

**Table 1**

| AC (Uniprot) | Protein name | Main functions & processes |
|---|---|---|
| P78417 | Glutathione S-transferase omega-1 | Oxidoreductase activity. |
| P11021 | 78 kDa glucose-regulated protein | Anti-apoptosis. Regulation of protein folding in ER. |
| P04179 | Superoxide dismutase [Mn], mitocondrial | Anti-apoptosis. Release of cytochrome c from mitochondria. |
| P11142 | Heat shock cognate 71 kDa protein | Chaperone. Repressor of transcriptional activation. |
| P36871 | Phosphoglucomutase-1 | Breakdown and synthesis of glucose. |
| O00469 | Procollagen-lysine,2-oxoglutarate 5-dioxygenase 2 | Extracellular matrix organization. |
| P04632 | Calpain small subunit 1 | Extracellular matrix organization. |
| P60953 | Cell division control protein 42 homolog | Regulation of protein complex assembly. |
| Q96CG8 | Collagen triple helix repeat-containing protein 1 | Cell migration. |
| P02461 | Collagen alpha-1 (III) chain | Extracellular matrix organization. Negative regulation of neuron migration. |
| P07203 | Glutathione peroxidase 1 | Cellular response to reactive oxygen species. |
| Q13011 | Delta (3,5)-Delta(2,4)-dienoyl-CoA isomerase, mitochondrial | Lipid metabolism. |
| Q8IVL6 | Prolyl 3-hydroxylase 3 | Extracellular matrix organization. |
| P61981 | 14-3-3 protein gamma | Apoptotic process. Regulation of neuro differentiation. |
| O60664 | Perilipin-3 | Vesicle-mediated transport. |
| P47756 | F-actin-capping protein subunit beta | Cytoskeleton organization. |
| O14558 | Heat shock protein beta-6 | Response to stress. |
| P40121 | Macrophage-capping protein | Actin-binding. Protein complex assembly. |
| Q9UHL4 | Dipeptidyl peptidase 2 | Degradation of oligopeptides. |
| P14618 | Pyruvate kinase PKM | Glycolysis. Programmed cell death. |

**Supplementary Data (Figures)**

**Click here to download Supplementary Material: Supplementary Data (Figures).pdf**

**Supplementary Data S4**

**Click here to download Supplementary Material: Supplementary Data S4.docx**

**Supplementary Data S6**

**Click here to download Supplementary Material: Supplementary Data S6.docx**

**Supplementary Data S8**

**Click here to download Supplementary Material: Supplementary Data S8.xlsx**